ARTICLE NO. 78-1223

Theoretical and Experimental Study of the Drag of Single- and Multielement Airfoils

Lawrence E. Olson*
NASA Ames Research Center, Moffett Field, Calif.
William D. James†
Iowa State University, Ames, Iowa
and
Phillip R. McGowan‡
Computer Sciences Corporation, Mountain View, Calif.

The viscous/potential flow past single-element and multielement airfoils is studied theoretically and experimentally. A computerized analysis, based on iteratively coupled potential-flow and boundary-layer analysis, is used to predict the flowfield of the airfoil. The method yields detailed characteristics of conventional laminar and turbulent boundary layers, turbulent wakes, and confluent boundary layers. The viscous flows are analyzed with a method that uses finite-difference solutions of the boundary-layer equations. Reynolds stress in the boundary layers and wakes is simulated with eddy viscosity models for the various zones. The viscous calculations are carried into the wake of the airfoil where the drag is found from the defect in the wake momentum.

Nomenclature

c = airfoil reference chord
C_l = airfoil lift coefficient, airfoil lift/$(1/2)\rho u_\infty^2 c$
C_d = airfoil drag coefficient, airfoil drag/$(1/2)\rho u_\infty^2 c$
d = wake thickness
H = height of test section of wind tunnel
L = mixing length
p = static pressure
q_∞ = free-stream dynamic pressure, $(1/2)\rho u_\infty^2$
Re = reference chord Reynolds number, $\rho u_\infty c/\mu$
R_θ = momentum thickness Reynolds number, $\rho u_\infty \theta/\mu$
s = distance along airfoil surface or wake streamline, measured from stagnation point
u = s-direction velocity component in boundary-layer coordinate system
u_∞ = freestream velocity
v = y-direction velocity component in boundary-layer coordinate system
x,z = airfoil coordinates
y = boundary-layer coordinate orthogonal to airfoil surface or orthogonal to wake streamline
α = angle of attack, deg
γ = intermittancy factor [see Eq. (7)]
δ_f = flap deflection, deg
δ^* = boundary-layer displacement thickness, $(1/u_e)\int_0^\infty (u_e - u)\,dy$
ϵ = eddy viscosity
η = transformed boundary-layer coordinate, $(u_e/\nu\sqrt{2\xi})y$
θ = boundary-layer momentum thickness, $(1/u_e^2)\int_0^\infty u(u_e - u)\,dy$
ν = kinematic viscosity
ξ = transformed boundary-layer coordinate, $(1/\nu)\int_0^s u_e\,ds$
ρ = fluid density

Subscripts

e = edge of boundary layer
l = lower surface
max. = maximum
u = upper surface
∞ = freestream

I. Introduction

WINGS with trailing-edge flaps and leading-edge slats are commonly used to obtain the lift required for landing and takeoff of modern fixed-wing aircraft. At present, the theoretical design of these high-lift systems is based primarily on the analysis of the two-dimensional viscous flow about multielement airfoils. At angles of attack below stall, these two-dimensional methods can usually adequately predict airfoil lift and pitching moment characteristics. The calculation of lift is primarily an inviscid problem requiring only a viscous correction for boundary-layer displacement and entrainment effects. In contrast, the prediction of drag with comparable accuracy is more formidable because airfoil drag, a direct result of viscous phenomena, depends primarily on the accurate prediction of the details of the laminar and turbulent viscous flow and the interaction of the viscous flow with the inviscid flow. For example, multielement airfoils characteristically have a drag force smaller by one to two orders of magnitude than the lift force. As a result, the drag force calculation requires much greater resolution to achieve an equivalent accuracy.

Two basic approaches are used to calculate multielement airfoil drag. In the first method, based on the integration of the surface pressure and skin-friction distributions around the contours of the various airfoils, the net pressure drag and skin-friction drag forces are summed to get the total profile drag; in the second method, based on the calculation of the total momentum defect at some location in the airfoil wake, the momentum defect equals the total profile drag. The ac-

Presented as Paper 78-1223 at the AIAA 11th Fluid and Plasma Dynamics Conference, Seattle, Wash., July 10-12, 1978; submitted Oct. 26, 1978. This paper is declared a work of the U.S. Government and therefore is in the public domain.

Index categories: Aerodynamics; Jets, Wakes, and Viscid-Inviscid Flow Interactions; Subsonic Flow.

*Aerospace Engineer. Member AIAA.
†Associate Professor. Member AIAA.
‡Senior Member of Technical Staff.

curacy of the pressure/skin-friction integration approach is severely limited by the accuracy with which the surface pressure integrations can be performed (for an example, Smith and Cebeci[1]). Although the wake-momentum defect method does not have this problem, other complications are introduced by the need for accurate knowledge of the wake-flow characteristics.

A momentum-defect method developed by Squire and Young[2] requires a knowledge of the shape factor $H=\delta^*/\theta$ and the momentum thickness θ of the boundary layers at the trailing edge of the airfoil. With this information, and a relationship between H and the static pressure in the wake (which was derived from a correlation with a data set from one single-element airfoil), the momentum defect in the far wake is determined. Smith and Cebeci[1] improved the accuracy for single-element airfoils by continuing the viscous calculation a short distance into the wake before applying the formula of Squire and Young. Goradia and Lilley[3] also developed a momentum-defect method to predict profile drag of single-element airfoils. Although viscous wake characteristics are computed, the technique is similar to that of Squire and Young since it uses a generalized parametric formula for the pressure distribution in the wake, i.e., a relationship derived by correlation with experiment. The results show that extending the viscous calculation into the wake improves the accuracy of the drag prediction.

Other investigators have found that a direct extension of the method of Squire and Young to multielement airfoils does not produce acceptable results (e.g., Olson and Dvorak,[4] Brune and Manke,[5] and Goradia and Cowell[6]). Because of the relative success in using defect methods for single-element airfoils, a similar extension of the viscous calculation into the wake appears the most promising for predicting the drag of multielement airfoils. This approach is the basis of the theoretical treatment presented in this report.

II. Theoretical Method

The theoretical method consists of iteratively coupled potential-flow, boundary-layer, and viscous-wake analyses. Except for a compressibility correction in the potential-flow calculation, the analysis assumes that the effects of compressibility are negligible.

Potential-Flow Analysis

In the potential-flow anlaysis, each element is represented by a closed polygon of planar panels connecting up to 80 input pairs. The vorticity distribution, which varies linearly along each panel, is continuous across the panel corner points. Thus, for n panels, $n+1$ unknowns are to be determined. The boundary condition (no flow through the surface, applied at each of the panel centers) provides n linear algebraic equations. An additional equation, used to close the system, specifies that the upper- and lower-surface velocities have a common limit at the trailing edge (i.e., the Kutta condition). For the case of an airfoil with a sharp trailing edge, the vorticity goes to zero because the trailing edge then becomes a stagnation point. In this case, an alternate Kutta condition is used to specify that the vorticity vanishes at the trailing edge on both the upper and lower surfaces. To complete the system of equations, a constant strength source distribution is located on the airfoil contour. Additional details on the potential-flow method of analysis are found in Olson and Dvorak.[4]

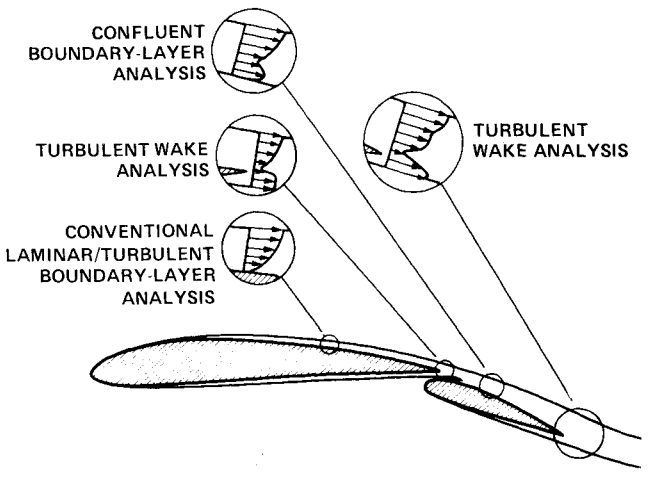

Fig. 1 Theoretical model of viscous flow.

Overview: Viscous-Flow Analysis

As illustrated in Fig. 1, viscous calculations are separated into three types of flows: conventional boundary layers, turbulent wakes, and confluent boundary layers, (i.e., wakes merging with conventional boundary layers). To obtain a complete viscous calculation, the conventional boundary layers on the upper and lower surfaces of the main airfoil are first analyzed. These calculations provide the initial conditions to start the turbulent-wake analysis at the trailing edge of the main component. This calculation continues downstream along a potential-flow streamline until the wake merges with the outer edge of the boundary layer on the upper surface of the flap (Fig. 2). At this point, the wake of the main element and the boundary layer on the flap combine into a single layer (a so-called confluent boundary layer) and the analysis continues stepwise downstream to the flap trailing edge. At the flap trailing edge, this confluent boundary-layer solution from the upper surface of the flap combines with the boundary-layer velocity profile from the lower surface of the flap and the calculation extends into the wake along a potential-flow streamline. The theoretical analysis of all three of these types of flows is based on the Levey-Lees form of the boundary-layer equations. Numerical solutions of these equations are obtained using the computationally efficient finite-difference method of Blottner.[7] Initial conditions, boundary conditions, and Reynolds stress models required to determine the structure of the various zones of flow are described briefly in the following sections. A detailed discussion of these analyses is presented in Ref. 7.

Conventional Boundary-Layer Analysis

The stagnation-point solution to the laminar boundary-layer equations forms the initial conditions for the conventional boundary-layer analysis. The boundary conditions on velocity and pressure at the outer edge of the viscous layer are obtained from the potential flow. A two-layer eddy-viscosity model, which is based on the recommendations of Cebeci[8] and Cebeci, Kaups, Mosinskis, and Rehn,[9] deter-

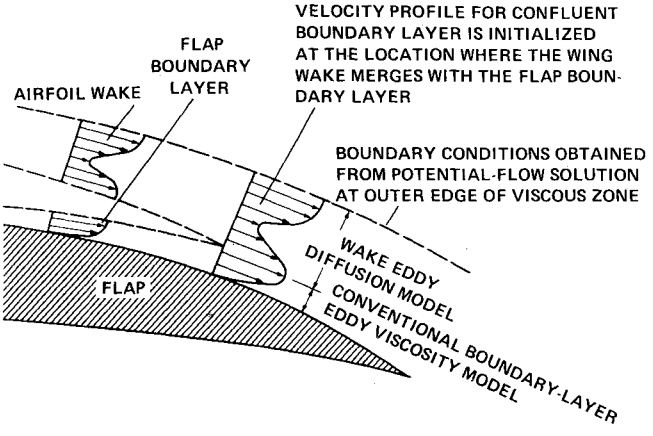

Fig. 2 Merging of the wake from the main airfoil with the boundary layer on the flap to form the confluent boundary layer on the upper surface of the flap.

mines the Reynolds stress characteristics of the transitional and turbulent boundary layers. In the inner region of the boundary layer, the eddy viscosity is denoted by ϵ_i and in the outer region by ϵ_0 where

$$\epsilon=\epsilon_i=L^2\left|\frac{\partial u}{\partial y}\right|\gamma_{tr} \quad \text{for } \epsilon_i\leq\epsilon_0 \tag{1}$$

and

$$\epsilon=\epsilon_0=\alpha u_e\delta^*\gamma_{tr} \quad \text{for } \epsilon_0<\epsilon_i \tag{2}$$

L is the mixing length and γ_{tr} is a parameter used to control the Reynolds stress during transition.

The correlations of Smith[10] are used to determine the point of laminar instability, and when laminar separation is detected the correlation of Gastor[11] is used to determine whether turbulent reattachment occurs. The computing time for one boundary-layer solution averages approximately 0.15 s on the CDC 7600 computer.

Viscous Wake Analysis

The viscous wake characteristics are found by solving the boundary-layer equations with the boundary-layer s-coordinate (or ξ-coordinate) aligned with a potential-flow streamline. This streamline is located by a streamline trace starting at the trailing edge of the component under consideration (Fig. 3). The velocity profiles for the initial conditions for the wake are found from the upper- and lower-surface boundary-layer profiles. The boundary conditions on the u-velocity and on the static pressure are determined from the potential-flow velocity at the physical edges of the wake (Fig. 3). The static pressure gradient at the upper edge of the wake is not necessarily equal to that at the lower edge. This variation in pressure gradient is accounted for by assuming that the pressure gradient varies linearly with y from the potential-flow value at the lower edge of the wake to the potential-flow value at the upper edge. The third boundary condition in the wake requires that the viscous flow be aligned with the potential-flow streamline, that is,

$$v=0 \text{ at } \eta=0 \tag{3}$$

where η is the transformed boundary-layer coordinate normal to the wake streamline.

The wake eddy-viscosity model is a modification of the diffusion equation model first suggested by Goldberg[12] and later developed by Dvorak[13] and Dvorak and Woodward.[14]

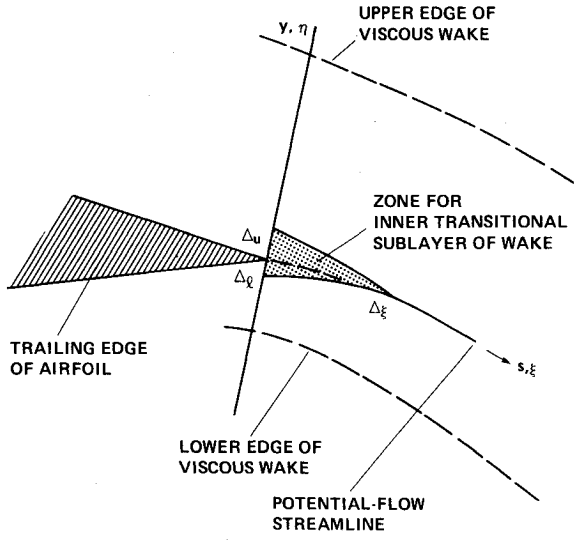

Fig. 3 Details of turbulent wake at the airfoil trailing edge.

The diffusion equation

$$\frac{\partial\epsilon_{\max.}}{\partial s}=\frac{k_1}{d}(\epsilon_l-\epsilon_{\max.}) \tag{4}$$

is used to account for the upstream history effects in the wake. Dvorak[13] suggests that k_1 be set to 0.02 for the analysis of turbulent boundary layers and to 0.20 for turbulent wall jets. In the present work, a value of 0.05 is used in all calculations. This value is based on the correlation of theoretically predicted Reynolds stress with the experimental measurements of Chevray and Kovasznay[15] for the turbulent wake of a flat plate. The parameter ϵ_l is the local equilibrium eddy viscosity, which is related to an eddy Reynolds number C defined as

$$C=\frac{u_d\sigma}{\epsilon_l}=14.5 \tag{5}$$

where u_d is the velocity defect and the constant σ has a value of 0.127.

The eddy-viscosity distribution across the wake is given by

$$\epsilon=\gamma\epsilon_{\max.} \tag{6}$$

where γ is an intermittency factor defined by

$$\gamma=\left[1+5.5\left(\frac{y-y_m}{y_e-y_m}\right)^6\right]^{-1} \tag{7}$$

The term y_m is the value of y at the point where the u-component of velocity is minimal; y_e is the value of y at the point where the velocity is 99% of the velocity at the edge of the wake. To start the wake integration requires an initial value for $\epsilon_{\max.}$ in Eq. (4). This initial value is obtained by setting $\epsilon_{\max.}$ equal to the maximum eddy viscosity in the upper surface boundary-layer profile at the trailing edge of the wing. In this way, the eddy viscosity in the wake is coupled with the dominant viscous layer on the airfoil. For more than one distinct wake (such as the flow in the wake of the flap in Fig. 1), the foregoing eddy viscosity model is applied to each wake.

Beginning a wake calculation at an airfoil trailing edge requires special treatment because of the abrupt release in the surface boundary condition ($u=0$) as the flow moves from the trailing edge of the airfoil into the wake. As a result, the

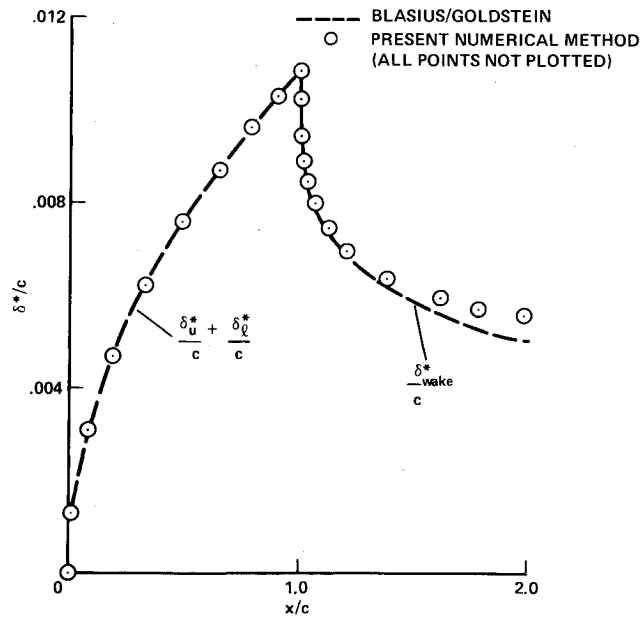

Fig. 4 Boundary-layer and wake displacement thickness for the laminar flow about a flat plate, $Re=10^5$.

gradients in the streamwise direction become large in the immediate vicinity of the trailing edge of the airfoil. Although these large gradients do not cause any noticeable numerical problem for laminar flows, they can prevent the reliable starting of turbulent wake calculations. This difficulty is attributed to the combined effect of large gradients in the turbulent velocity profiles and large Reynolds stresses associated with the wake eddy-viscosity model described in the previous paragraphs.

A numerically reliable method has been developed, based on a more realistic Reynolds stress model for the immediate vicinity of the trailing edge of the airfoil. The eddy diffusion model incorporates a transitional sublayer model shown schematically in Fig. 3. The sublayer provides a limited region in the near-wake of the airfoil where the Reynolds stress distribution is forced to make a gradual transition to the fully turbulent flow described by the wake eddy diffusion model. The distance this sublayer extends above the airfoil trailing edge Δ_u is set equal to the thickness of the inner region (as defined by the point where ϵ_i equals ϵ_0) of the upper-surface boundary layer at the trailing edge of the main element. The distance the wake sublayer extends below the trailing edge of the airfoil Δ_l is similarly determined using the properties of the boundary layer on the lower surface. The distance over which the sublayer zone extends into the wake Δ_ξ is set to $5(\Delta_u+\Delta_l)$. The Reynolds stress in the sublayer is then expressed as

$$\epsilon=\epsilon_l\left[1-\left(\frac{\xi-\xi_{te}}{\Delta_\xi}\right)\left(\frac{\eta}{\Delta_u}\right)+\left(\frac{\xi-\xi_{te}}{\Delta_\xi}\right)\right]$$

$$\text{for} \quad \begin{cases} 0\le\eta\le\Delta_u \\ \xi_{te}\le\xi\le\xi_{te}+\Delta_\xi \end{cases} \tag{8}$$

and

$$\epsilon=\epsilon_l\left[1-\left(\frac{\xi-\xi_{te}}{\Delta_\xi}\right)\left(\frac{\eta}{\Delta_l}\right)+\left(\frac{\xi-\xi_{te}}{\Delta_\xi}\right)\right]$$

$$\text{for} \quad \begin{cases} 0\le\eta\le\Delta_l \\ \xi_{te}\le\xi\le\xi_{te}+\Delta_\xi \end{cases} \tag{9}$$

The foregoing modification to the wake diffusion model and the incorporation of the automated finite-difference mesh generation scheme described in a following section greatly improves the reliability of the Blottner finite-difference solution technique near airfoil trailing edges.

Confluent Boundary-Layer Analysis

The analysis of the confluent boundary layer is initiated at the location where the wake of the main element merges with the boundary layer on the upper surface of the flap. The initial conditions are obtained by resolving the wake velocity components into the boundary-layer coordinate system of the flap upper surface. The location of the merge point is based on the computed intersection of the lower edge of the wake and the outer edge of the flap boundary layer. Because of the relatively large thickness of the confluent boundary layers, the boundary condition should be evaluated at the edge rather than at the airfoil surface. The calculations assume that the static pressure does not vary across the confluent boundary layer.

The eddy-viscosity model for the confluent boundary layer combines the conventional boundary-layer and the wake model described earlier. As shown in Fig. 2, the eddy diffusion model is used for the wake region of the confluent boundary layer; the two-layer conventional boundary-layer model is used in the wall region. The initial value for $\epsilon_{max.}$ in the wake region of the confluent boundary layer is obtained by equating it to $\epsilon_{max.}$ obtained from the wing-wake calculation at the merge point. This technique couples the Reynolds stress characteristics in the confluent boundary layer with those in the wake of the airfoil and accounts for upstream history effects on the Reynolds stress.

Finite-Difference Grid for Viscous Flows

The present method generates special finite-difference meshes to solve the boundary-layer equations for the various flows. The grid in the ξ-direction (along the airfoil surface or along a wake streamline) is determined by the static pressure distribution. The density of points is directly proportional to the local pressure gradient. Calculations for adverse pressure gradients generally require a denser mesh than favorable pressure gradients; therefore, regions of adverse pressure gradients are assigned a weighting factor of 4 above that assigned to favorable pressure gradients. Typically, 60 points in the ξ-direction are used for a boundary-layer solution, and 100 points are used for a wake analysis.

The grid in the η-direction (normal to the airfoil surface or normal to a wake streamline) is generated by two different techniques. The conventional boundary-layer analysis uses the geometrically expanding grid described by Cebeci.[8] Most calculations require only 16 to 24 points across the boundary layer to obtain numerically accurate solutions. For confluent boundary layers and wakes, the η-grid is based upon the local velocity profiles. The density of points is directly proportional to the local curvature of the u-velocity profile. As a result, regions of large curvature, such as those near the centerline of a wake, have a finer mesh than regions of low curvature, such as those near the edges of the wake. Typically, 30 to 50 points in the η-direction give good numerical accuracy.

Drag Calculation

Drag is computed from the momentum defect in the wake at a distance of 0.5 to 2.0 chords downstream of the airfoil trailing edge. The formula of Betz

$$C_d=\int_{\text{wake}}\left[\frac{p_{t_\infty}-p_t}{q_\infty}\right]d\left(\frac{y}{c}\right)+\int_{\text{wake}}\left[\left(\frac{p_{t_\infty}-p}{q_\infty}\right)^{1/2}-\left(\frac{p_t-p}{q_\infty}\right)^{1/2}\right]\left[\left(\frac{p_{t_\infty}-p}{q_\infty}\right)^{1/2}+\left(\frac{p_t-p}{q_\infty}\right)^{1/2}-2\right]d\left(\frac{y}{c}\right) \tag{10}$$

is integrated numerically using data from the viscous wake calculation. To evaluate the integrand of Eq. (10), the static pressure is assumed to vary linearly between the potential-flow pressure at the lower and upper edge of the wake.

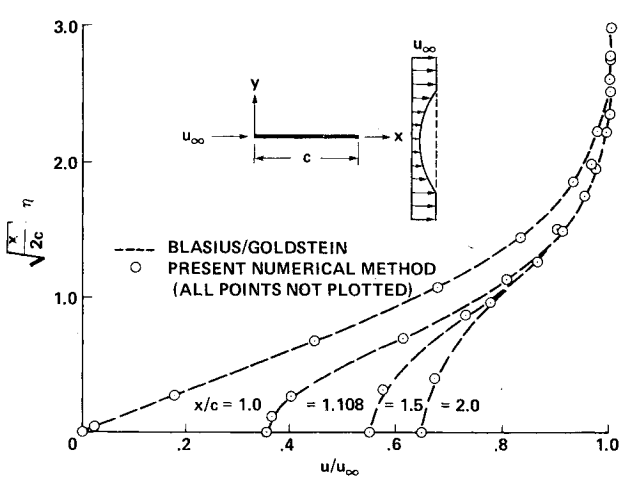

Fig. 5 Velocity profiles for the laminar flow in the wake of a flat plate, $Re=10^5$.

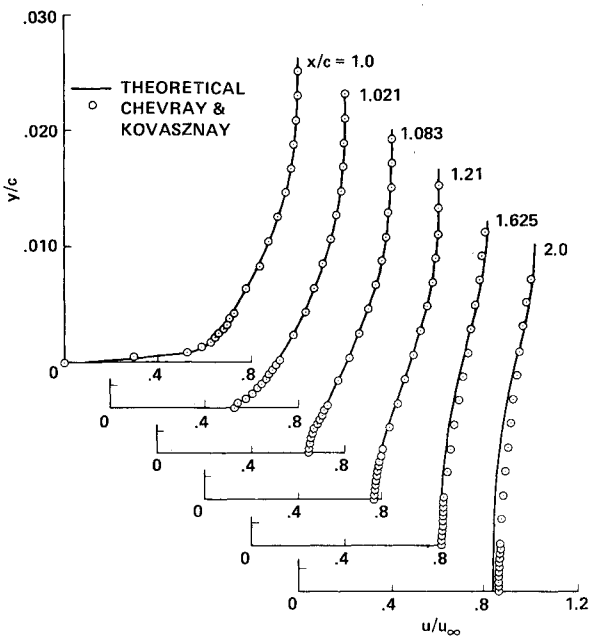

Fig. 6 Velocity profiles for the turbulent flow in the wake of a flat plate, $Re = 0.655 \times 10^6$.

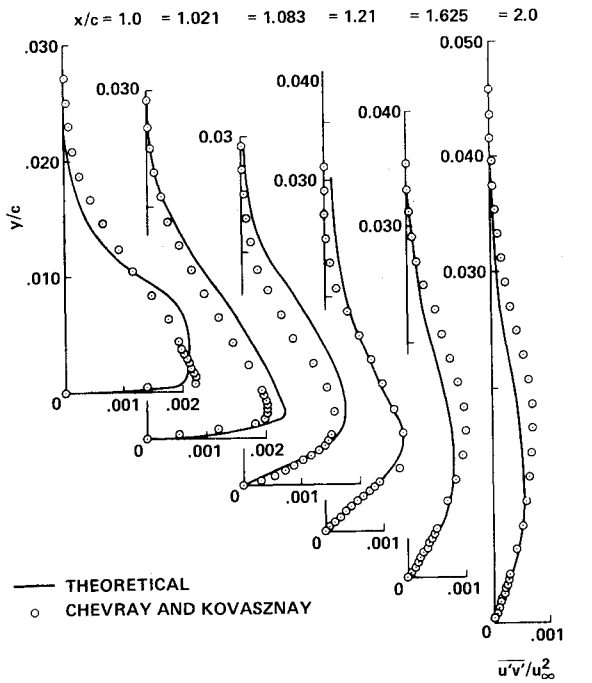

Fig. 7 Reynolds stress profiles for the turbulent flow in the wake of a flat plate, $Re = 0.655 \times 10^6$.

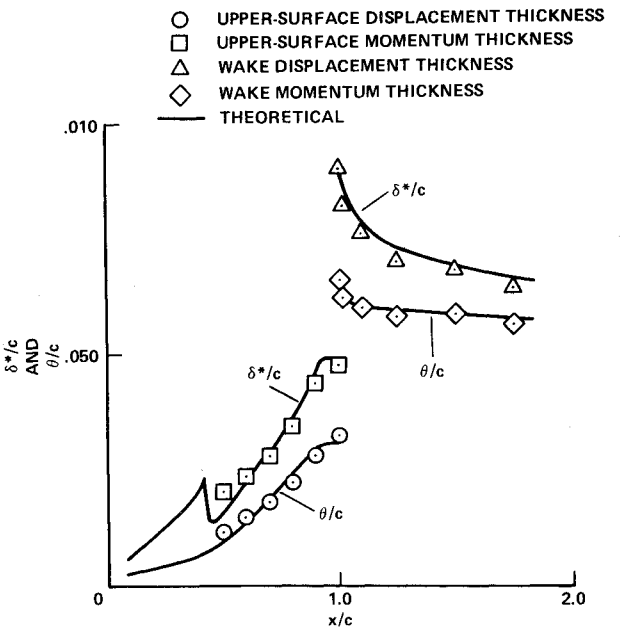

Fig. 8 Momentum thickness and displacement thickness for the boundary layer and wake of a Joukowski airfoil, $\alpha = 0$ deg, $Re = 4.2 \times 10^6$.

Viscous/Inviscid Coupling

The effect of boundary-layer displacement and mass entrainment on the potential-flow field is simulated by piecewise linear source distributions on the panels describing the airfoil contour. The strength of these source panels is determined directly from the boundary-layer solution as $q = \mathrm{d}(u_e \delta^*)/\mathrm{d}s$ where u_e is the potential-flow velocity at the edge of the boundary layer and δ^* is the boundary-layer displacement thickness. In the potential-flow analysis, a modified Kutta condition requires that the flow be tangent to the panels at the trailing edge on the upper and lower surfaces. The boundary condition on the surface panels requires that the velocity normal to the surface equals the strength of the known source distribution. These conditions uniquely determine the potential-flow solution; the resulting pressure field is used in subsequent boundary-layer, wake, and confluent boundary-layer analyses.

III. Comparison of Theory and Experiment

Blottner[7] demonstrated the accuracy of the finite-difference method for several conventional laminar and turbulent boundary-layer flows. Of particular interest for the present work is the accuracy of the numerical technique when extended to laminar and turbulent wake flows and the testing of the validity of the wake eddy-diffusion model. Thus, the theoretical results of the present method are compared with exact theoretical solutions and experimental measurements for a flat-plate airfoil and a single-element airfoil. These comparisons are then followed by a comparison of the theoretical predictions with the experimental data for a two-element configuration.

Laminar and Turbulent Flow over a Finite Flat Plate

The first comparisons use the Blasius solution for the laminar boundary layer on a flat plate combined with the Goldstein solution for the laminar wake downstream of the flat plate.[16] Figures 4 and 5 compare the finite-difference solutions of the boundary-layer and wake equations with the solutions of Blausius and Goldstein. Displacement thickness (Fig. 4) and detailed velocity profiles (Fig. 5) will agree well both on the plate and in the wake.

The second test uses the data of Chevray and Kovasznay[15] for the mean velocity and the Reynolds stress for the turbulent flow in the vicinity of the trailing edge of a flat plate. These comparisons verify the accuracy of the numerical method when applied to turbulent wake flows and show that the eddy diffusion model is valid for the calculation of Reynolds stress in turbulent wakes.

The theoretical results in Figs. 6 and 7 are taken from a complete laminar/transitional/turbulent boundary-layer and wake calculation at Reynolds number 0.655×10^6. The computed momentum thickness at the trailing edge of the plate was forced to equal the experimental value by fixing the location of laminar instability at $x/c = 0.25$. The mean velocity profiles in Fig. 6 are in good agreement although the present method predicts slightly higher centerline velocities near the plate trailing edge ($s/c = 1.021$, 1.083). The shape of the Reynolds stress profiles and the location (y/c) of the

maximum Reynolds stress (Fig. 7) are nearly the same for predicted and measured Reynolds stress characteristics. Therefore, the numerical technique is judged reliable and the eddy diffusion model being used for turbulent wakes is deemed satisfactory for predicting the Reynolds stresses.

Joukowski Airfoil

The flat-plate studies described above do not include the effect of a streamwise pressure gradient on the boundary-layer and wake flow structure. The experimental work of Preston and Sweeting[17] on a Joukowski airfoil documents boundary-layer and wake properties for a configuration in which the pressure gradient has an important if not dominant effect on the viscous flow. Figure 8 compares the measured and predicted displacement and momentum thicknesses on a Joukowski airfoil at an angle of attack of 0 deg. Both the boundary-layer characteristics on the airfoil and the viscous wake show good agreement. Figure 9 compares in detail the wake velocity profiles for several locations at (and downstream from) the trailing edge of the airfoil. Although the theory tends to predict a slightly lower rate of diffusion in the far wake ($x/c \geq 0.10$), the general agreement is good. Figure 10 compares the measured drag of Preston and Sweeting[17] with the drag predicted by the present analysis for angles of attack from 0 deg to 9 deg. As in the experiments, the calculations include natural transition as well as the case where the boundary layer on the upper and lower surfaces is tripped at $x/c = 0.05$. The agreement is reasonably good with the largest differences occurring at $\alpha = 9$ deg, at which incipient flow separation increases the drag. This is not taken into account by the theoretical method.

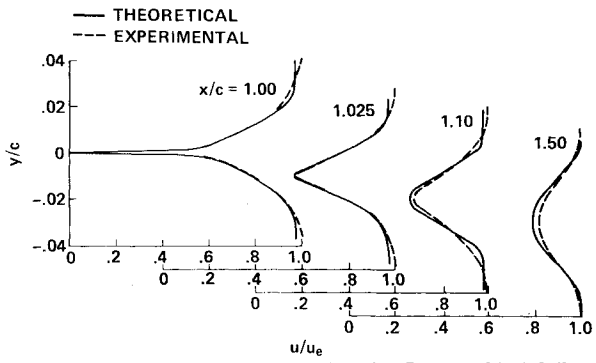

Fig. 9 Velocity profiles for the wake of a Joukowski airfoil, $\alpha = 0$ deg, $Re = 4.2 \times 10^6$.

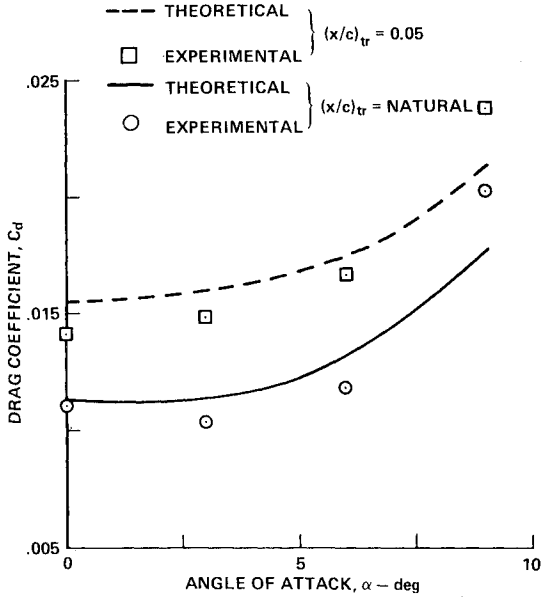

Fig. 10 Drag versus angle of attack for a Joukowski airfoil, $Re = 4.2 \times 10^6$.

NACA 4412 with Single-Slotted Flap

This subsection presents a comparison of the theoretical results with experimental data obtained on a two-element airfoil (Fig. 11). The deflection of the single-slotted flap was 10 deg and the test was conducted at a Reynolds number of 4.1×10^6. The airfoil configuration and test setup were designed to provide detailed experimental data which are not affected by flow separation on the upper or lower surfaces of either element. Static pressure and total pressure distributions in the wake of the airfoil were measured using an 81 tube wake rake. Data from the wake rake were integrated numerically using Eq. (10) to determine the total profile drag of the airfoil. Airfoil lift was obtained by integrating the surface pressure measured on the centerline of the model.

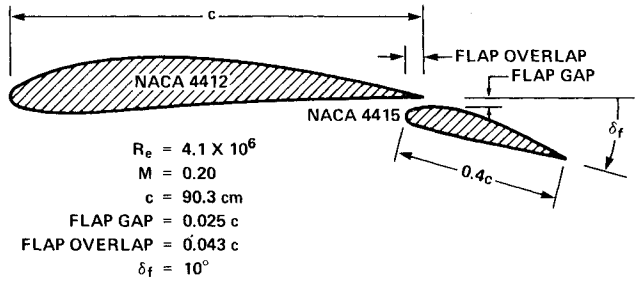

Fig. 11 Geometry definition and test conditions for two-element airfoil tested in the 7- by 10-ft wind tunnel operated by the Aeromechanics Laboratory, U.S. Army Research and Technology Laboratories.

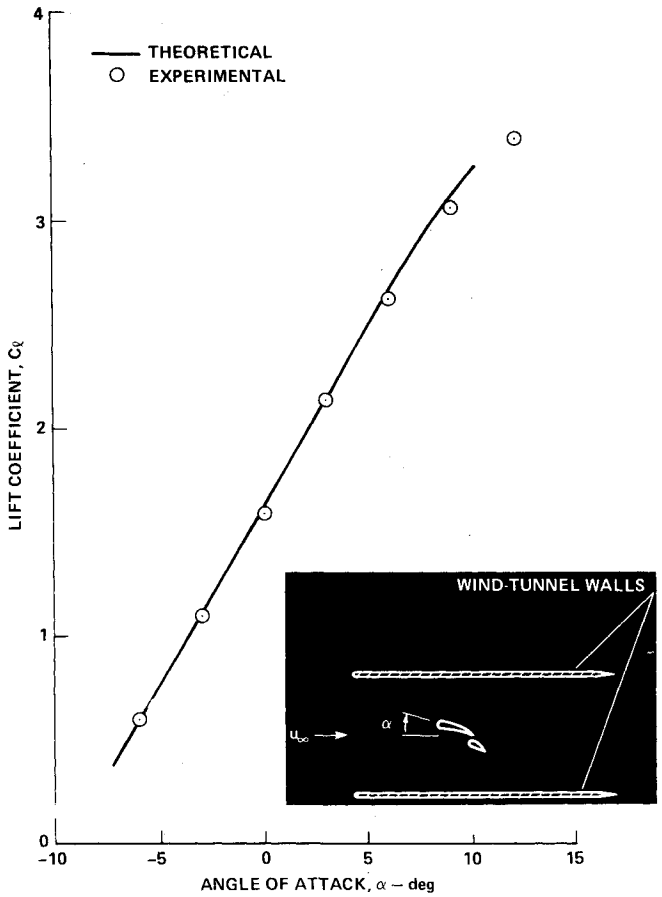

Fig. 12 Comparison of theoretical and experimental lift for NACA 4412 airfoil equipped with a single-slotted flap deflected 10 deg, flap gap = 0.025 chord, $Re = 4.1 \times 10^6$.

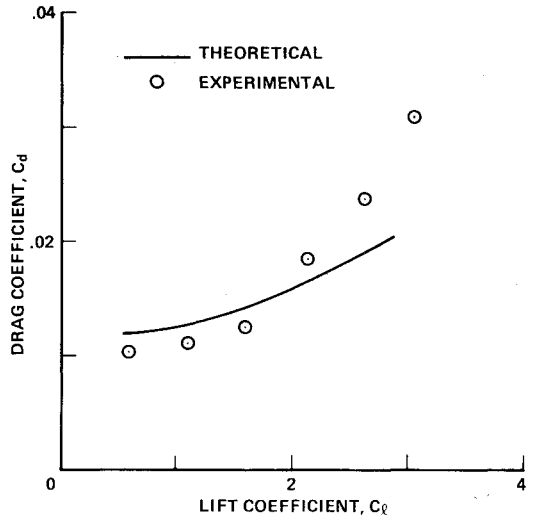

Fig. 13 Comparison of theoretical and experimental drag for NACA 4412 airofil equipped with a single-slotted flap deflected 10 deg, flap gap = 0.025 chord, $Re = 4.1 \times 10^6$.

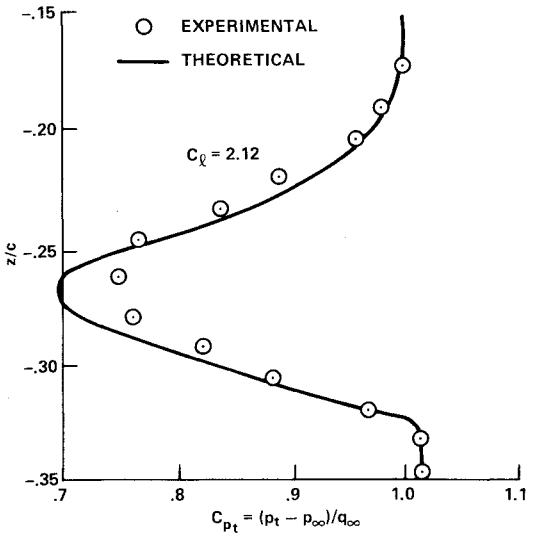

Fig. 14 Comparison of theoretical and experimental total pressure profiles in the wake of an NACA 4412 airfoil equipped with a single-slotted flap deflected 10 deg, flap gap = 0.025 chord, $Re = 4.1 \times 10^6$.

This wind-tunnel model provided high quality two-dimensional flow up to lift coefficients of three as was verified by: 1) comparison of chordwise pressure distributions obtained at spanwise locations of 0.55 chord on each side of the centerline of the model, with pressure distributions obtained on the model centerline; and 2) comparison of total profiles in the wake of the airfoil obtained at several spanwise locations.

The two-element airfoil was relatively large ($H/c = 3.4$) when compared with the wind-tunnel test section. When such a large model is tested with high lift coefficients ($C_l = 1.0$ to 3.0), a significant interaction occurs between the wind-tunnel walls and the flow around the airfoil. Rather than correct the experimental data to free-air conditions, the comparison between theory and experiment was thought to be more meaningful if the effects of the wind-tunnel walls were included in the theoretical calculations. Therefore, the wind-tunnel walls were simulated as thin plates ($t/c = 0.001$) that extended 1.35 chords upstream and 3.7 chords downstream of the airfoil. These limits correspond approximately to the beginning of the wind-tunnel bellmouth upstream of the airfoil and the beginning of the wind-tunnel diffuser downstream of the airfoil. The tunnel-wall geometry included a small (0.9 deg) diffusion angle. The viscous flows on both wind-tunnel walls were analyzed to take into account the displacement effects of the tunnel-wall boundary layers. The comparison in Fig. 12 of the predicted and experimentally measured lift shows the accuracy of this simulation.

Figure 13 compares computed and measured drag when the flap is deflected 10 deg and Reynolds number is 4.1×10^6. The flap gap, set at 0.025 chord was sufficiently large so that no more than a weak interaction existed between the wing wake and the flap upper-surface boundary layer. The agreement between theory and experiment is within 15% for lift coefficients of 0.6 to 2.2. Figure 14 compares the predicted and measured stagnation pressure across the wake at a distance 2.25 chords downstream of the trailing edge of the main airfoil. At this location the wake from the two airfoil components has merged into a single wake. The overall wake width and shape is predicted with good accuracy, although the predicted minimum velocity is slightly lower than the experimental value.

IV. Concluding Remarks

A theoretical method for analyzing viscous/potential flow around multielement airfoils has been described. Emphasis was placed on analyzing turbulent wakes and confluent boundary layers so that the flow structure could be determined with sufficient detail and accuracy to predict profile drag by the momentum defect in the wake. In support of the theoretical program, an experimental study was conducted in the 7- by 10-ft wind tunnel operated by the Aeromechanics Laboratory, U.S. Army Research and Technology Laboratories. Comparison of the present theory with this data and other experimental results led to the following conclusions:

1) Adding a transitional sublayer-model for the turbulent Reynolds stress in the vicinity of sharp trailing edges of airfoils greatly improved the reliability of the finite-difference analysis of turbulent wake flows.

2) The laminar and turbulent boundary-layer flow around a flat plate was predicted accurately. Comparing the present method with the Blasius/Goldstein laminar flow solution demonstrated that good numerical accuracy is obtainable with the finite-difference method and the automated grid generation techniques used here. The turbulent-flow analysis not only showed that the mean velocity profiles on the plate and in the wake were in good agreement with experiment but also that the wake Reynolds stress relationship adequately modeled the effects of turbulence.

3) Measurements by Preston and Sweeting[17] of the drag, boundary-layer, and wake characteristics of a Joukowski airfoil were accurately represented by the present method for angles of attack up to incipient flow separation.

4) The drag predicted for a two-element configuration agrees reasonably well with experiment for lift coefficients of 0.6 to 2.2.

Although the present study made only limited comparisons between theory and experiment for the characteristics of multielement airfoils, the theoretical method was fundamentally sound, computationally efficient, and sufficiently flexible to serve as a basic model for continued research. Future efforts should consider configurations with higher angles of attack and greater flap loadings, and configurations that emphasize the merging of the wing wake with the boundary layer on the flap. Whenever possible, future comparisons between theory and experiment should also include the Reynolds stress characteristics for turbulent wakes and confluent boundary layers.

References

[1]Smith, A.M.O. and Cebeci, T., "Remarks on Methods for Predicting Viscous Drag," AGARD-CP-124, Aerodynamic Drag, Izmir, Turkey, April 10-13, 1973.

[2]Squire, H.B. and Young, A.D., "The Calculation of the Profile Drag of Airfoils," British Aeronautical Research Council, R&M 1838, 1937.

[3]Goradia, S.H. and Lilley, D.E., "Theoretical and Experimental Study of a New Method for Prediction of Profile Drag of Airfoil Sections," NASA CR-2539, June 1975.

[4]Olson, L.E. and Dvorak, F.A., "Viscous/Potential Flow about Multi-Element Two-Dimensional and Infinite Swept Wings: Theory and Experiment," presented as Paper 76-18 at the AIAA Aerospace Sciences Meeting, Washington, D.C., Jan. 26-28, 1976.

[5]Brune, G.W. and Manke, J.W., "A Critical Evaluation of the Prediction of the NASA-Lockheed Multielement Airfoil Computer Program," NASA CR-145322, March 1978.

[6]Goradia, S.H. and Cowell, G.T., "Analysis of High-Lift Wing Systems," *The Aeronautical Quarterly*, Vol. XXVI, May 1975, pp. 88-107.

[7]Blottner, F.G., "Investigation of Some Finite-Difference Techniques for Solving the Boundary-Layer Equations," *Computer Methods in Applied Mechanics and Engineering*, Vol. 6, 1975, pp. 1-30.

[8]Cebeci, T., "Calculation of Three-Dimensional Boundary Layers: I. Swept Infinite Cylinders and Small Cross Flows," *AIAA Journal*, Vol. 12, June 1974, pp. 779-786.

[9]Cebeci, T., Kaups, K., Mosinskis, G.J., and Rehn, J.A., "Some Problems of the Calculation of Three-Dimensional Boundary-Layer Flows on General Configurations," McDonnell Douglas Company Rept. MDC J5884, April 1973.

[10]Smith, A.M.O., "Transition, Pressure Gradient and Stability Theory," *Proceedings of 9th International Congress of Applied Mechanics*, Vol. 7, Brussels, 1957.

[11]Gastor, M., "The Structure and Behavior of Laminar Separation Bubbles," ARC Rept. 28-226, 1967.

[12]Goldberg, P., "Upstream History and Apparent Stress in Turbulent Boundary Layers," GTLR 85, MIT, Cambridge, Mass., 1966.

[13]Dvorak, F.A., "Calculation of Turbulent Boundary Layers and Wall Jets over Curved Surfaces," *AIAA Journal*, Vol. 11, April 1973, pp. 517-524.

[14]Dvorak, F.A. and Woodward, F.A., "A Viscous/Potential Flow Interaction Analysis Method for Multielement Infinite Swept Wings," NASA CR-2476, Vol. 1, Nov. 1974.

[15]Chevray, R. and Kovasznay, L.S.F., "Turbulence Measurements in the Wake of a Thin Flat Plate," *AIAA Journal*, Vol. 7, Aug. 1969, pp. 1641-1643.

[16]Schlichting, H., *Boundary Layer Theory*, McGraw-Hill, New York, 1960, Chap. 9.

[17]Preston, J.H. and Sweeting, N.E., "The Experimental Determination of the Boundary Layer and Wake Characteristics of a Simple Joukowski Aerofoil, with Particular Reference to the Trailing Edge Region," ARC Tech. Rept. R&M 1998, March 1943.